*Nat Chem Biol*. Author manuscript; available in PMC 2014 June 01.

Published in final edited form as:
*Nat Chem Biol*. 2013 December ; 9(12): . doi:10.1038/nchembio.1359.

# Development of small molecule inhibitors targeting adipose triglyceride lipase

**Nicole Mayer**[#1], **Martina Schweiger**[#2], **Matthias Romauch**[2], **Gernot F. Grabner**[2], **Thomas O. Eichmann**[2], **Elisabeth Fuchs**[1], **Jakov Ivkovic**[1], **Christoph Heier**[2], **Irina Mrak**[2], **Achim Lass**[2], **Gerald Höfler**[3], **Christian Fledelius**[4], **Rudolf Zechner**[2], **Robert Zimmermann**[2,*], and **Rolf Breinbauer**[1,*]

[1]Institute of Organic Chemistry, Graz University of Technology, 8010 Graz, Austria.

[2]Institute of Molecular Biosciences, University of Graz, 8010 Graz, Austria.

[3]Institute of Pathology, Medical University of Graz, 8010 Graz, Austria.

[4]Novo Nordisk A/S, Novo Nordisk Park, DK-2760 Måløv, Denmark

[#] These authors contributed equally to this work.

## Abstract

Adipose triglyceride lipase (ATGL) is rate-limiting in the mobilization of fatty acids from cellular triglyceride stores. This central role in lipolysis marks ATGL as interesting pharmacological target since deregulated fatty acid metabolism is closely linked to dyslipidemic and metabolic disorders. Here we report on the development and characterization of a small-molecule inhibitor of ATGL. Atglistatin is selective for ATGL and reduces fatty acid mobilization *in vitro* and *in vivo*.

White adipose tissue (WAT) functions as buffer for dietary lipids and stores excess energy in form of triacylglycerol (TG). TG mobilization (lipolysis) strongly depends on adipose triglyceride lipase (ATGL)[1] and its co-activator protein comparative gene identification 58[2] (CGI-58, also known as α/β hydrolase domain-containing 5). ATGL performs the first step in TG catabolism generating diacylglycerol[3] which is subsequently degraded by hormone-sensitive lipase (HSL) and monoglyceride lipase (MGL) into glycerol and fatty acids (FA)[4,5].

Within the last decades increasing evidence has emerged that FA metabolism is closely linked to the development of metabolic disorders. Increased WAT lipolysis, as observed in obesity, can promote lipid overload of non-adipose tissues such as liver, pancreas, skeletal and cardiac muscle. This is associated with impaired metabolic functions of these tissues, insulin resistance, and inflammation[6,7]. The adverse effects of ectopic lipid overload are summarized under the term “lipotoxicity”[8] and central in the pathogenesis of metabolic disorders. Since ATGL is rate-limiting in lipolysis, inhibition of this enzyme is probably the most efficient way to reduce FA mobilisation and thus might represent a strategy to

[*]Biological correspondence should be addressed to R. Zimmermann robert.zimmermann@uni-graz.at. [*]Chemical correspondence should be addressed to R. Breinbauer breinbauer@tugraz.at.

**Author contributions** Ro.Zi, R.B, Ru.Ze., G.H., C.F. conceived the study design. N.M., M.S., M.R., T.O.E., J.I., E.F., G.F.G., A.L., C.H., I.M. performed the experiments. Ro.Zi., R.B. analyzed the data and wrote the paper. All the authors read, revised, and approved the manuscript.

**Competing financial interests** N.M, M.S., M. R., Ro.Zi, and R.B. have filed for a patent.

**Additional information** Supplementary information and chemical compound information is available online. Correspondence and requests for materials should be addressed to Ro.Zi. (biological questions) and R.B. (chemical questions).


Europe PMC Funders Author Manuscripts

counteract lipotoxicity. Studies in genetically modified mice demonstrate that the loss of ATGL is associated with improved glucose tolerance and insulin sensitivity on a normal diet and under conditions of high-fat diet-induced insulin resistance[1,9,10]. Notably, insulin sensitivity and glucose tolerance are improved despite severe TG accumulation in non-adipose tissues suggesting that increased ectopic lipid storage *per se* does not cause lipotoxicity[1,11]. It is reasonable to assume that ATGL generates FAs promoting the synthesis of lipotoxic metabolites which have been associated with the development of insulin resistance, such as acyl-CoA[12], ceramides[13], and diglycerides[14].

Here we describe the identification and characterization of the first small molecule inhibitor of ATGL. Lead structures for ATGL inhibitors were available originating from a high throughput screen with the intention to identify HSL inhibitors[15,16]. Several compounds in this screen inhibited lipolysis in living cells but failed to inhibit HSL in enzyme assays. Subsequent enzyme activity assays confirmed that compound **1** (Fig. 1A) inhibits ATGL activity ($IC_{50}$ = 50 μM) and also represents a chemotype with the potential for fast optimization. Since compound **1** turned out to be cytotoxic and a likely subject of phase II metabolism, we set out to optimize our inhibitors and established a structure-activity relationship. Compunds **2**-**4** represent major milestones along this optimization effort, in which we identified electron-rich substituents in the bottom ring and the 1,3-substitution pattern in the top ring as important. When we surveyed possibilities to replace the ester moiety in the 3-position of **3** by other functional groups, we found that substitution with urea (compound **4**) showed highest ATGL inhibition potential ($IC_{50}$ = 0.7 μM, Fig. 1A). The dose-dependent inhibition of ATGL activity by compounds **3** and **4** is shown in Supplementary Results, Supplementary Fig. 1A. Cytotoxicity assays for compound **4** revealed virtually no toxicity up to a concentration of 50 μM (Supplementary Fig. 2). This compound appeared suitable as a chemical tool for detailed biological characterization and was named Atglistatin.

To determine the mechanism of Atglistatin-mediated ATGL inhibition, we performed inhibitor kinetic studies by varying substrate and inhibitor concentrations. Lineweaver-Burk analysis revealed an increase in $K_m$ values and unchanged $V_{max}$ indicating a competitive mechanism (Fig. 1B). Based on apparent $K_m$ values and using non-linear regression analysis (SigmaPlot 12.0), we calculated a $K_i$ value of 355 ± 48 nmol/l. Furthermore, Atglistatin inactivated ATGL in the presence and in the absence of CGI-58 (Supplementary Fig. 3A, B) and the inhibitor did not displace ATGL from lipid droplets of adipocytes (Supplementary Fig. 4A, B). Immunoprecipitation experiments revealed that Atglistatin does not interfere with the interaction of ATGL and its co-activator CGI-58 (Supplementary Fig. 4C). Altogether, these observations suggest that Atglistatin directly inhibits ATGL in a competitive manner.

To evaluate whether Atglistatin is specific for ATGL, white adipose tissue (WAT) lysates of wild-type and ATGL-deficient (ATGL-ko) mice were analyzed for TG hydrolase activity in the presence and absence of increasing concentrations of Atglistatin. As shown in Fig. 1C, Atglistatin inhibited TG hydrolase activity of wild-type WAT in a dose-dependent manner up to 78% at the highest concentration. In comparison to wild-type preparations, TG hydrolase activity in WAT lysates from ATGL-ko animals was reduced by approximately 70% and Atglistatin had only a moderate effect on the residual activity. The combined use of Atglistatin and the HSL inhibitor Hi 76-0079[17] led to an almost complete inhibition (-95%) of TG hydrolase activity of WAT which implicates that most of the non-ATGL activity can be ascribed to HSL (Supplementary Fig. 5). Substantial inhibition of TG hydrolase activity by Atglistatin and/or Hi 76-0079 was also observed in lysates of other tissues including brown adipose tissue (BAT), skeletal muscle (SM), cardiac muscle (CM), and liver, but not in tissue lysates of ATGL-ko mice (Supplementary Fig. 5). Furthermore,

enzyme assays revealed that Atglistatin does not inhibit HSL, MGL, pancreatic lipase, lipoprotein lipase, and two lysophospholipases of the patatin-like phospholipase domain containing protein family[18] (PNPLA) exhibiting homology to ATGL (PNPLA6 and PNPLA7; Supplementary Fig. 6). These results indicate that Atglistatin exhibits high selectivity for ATGL, does essentially not inhibit other key metabolic lipases, and is not a general inhibitor of PNPLA proteins.

Atglistatin was highly effective in inhibiting lipolysis in WAT organ cultures of wild-type mice. The release of the lipolytic parameters FA and glycerol was determined in the absence and in the presence of the adenylyl cyclase activator forskolin (basal and activated lipolysis, respectively). Basal release of FA and glycerol was reduced up to 64% and 43%, respectively (Fig. 1D, E). In the presence of forskolin, Atglistatin reduced FA release up to 72% and glycerol release up to 62% (Fig. 1 F, G). Fat pads from ATGL-ko mice exhibited reduced FA and glycerol release under basal and activated conditions (dashed line, Fig. 2A-D) as demonstrated previously[1] and, importantly, addition of Atglistatin did not affect lipolysis. Dose-dependent inhibition of basal and activated lipolysis by Atglistatin was also observed in 3T3-L1 adipocytes (Supplementary Fig. 7A, B). As a control we treated 3T3-L1 adipocytes with the close structural analog **5** of Atglistatin (insert Supplementary Fig. 8A). **5** poorly inhibited ATGL activity (dashed line, Supplementary Fig. 8A) in enzyme assays and did not lead to substantial inhibition of lipolysis (dashed line, Supplementary Fig. 8B, C). Collectively, these results suggest that Atglistatin inhibits lipolysis in cell and organ cultures by targeting ATGL.

Finally, we tested the *in vivo* potential of Atglistatin to inhibit lipolysis in fasted wild-type C57Bl/6J mice. Animals received **4** dissolved in olive oil by oral gavage. After application, blood and tissues were collected for determination of plasma parameters, tissue TG levels, and inhibitor concentrations. Time-course experiments revealed that the lipolytic parameters FA and glycerol were reduced 4 and 8 hours after application and returned to normal after 12 hours (Fig. 2A). Eight hours after treatment, we observed a dose-dependent decrease in FA and glycerol levels up to 50% and 62%, respectively (Fig. 2B). Atglistatin also caused a strong reduction in plasma TG levels (-43%) while blood glucose, total cholesterol, ketone bodies, and insulin levels did not significantly change (Supplementary Table 1A). Dose and time-dependent inhibition of lipolysis was also observed in response to intraperitoneal injection of Atglistatin (Supplementary Fig. 9A-B).

ATGL-deficiency is characterized by TG accumulation in multiple tissues which is most pronounced in the heart[1]. As shown in Fig. 2C, single inhibitor administration did not cause TG accumulation in all tissues investigated except liver. This suggests that long-term treatment or higher doses are required to elicit ectopic TG accumulation. Using MS analysis we found accumulation of Atglistatin in liver, WAT, and BAT. Other tissues, including brain, kidney, CM, SM, and lung, accumulated comparably low amounts of Atglistatin (Fig. 2D). This implicates that also differential tissue distribution affects inhibitor activity and might explain the lack of lipid accumulation in cardiac muscle and other tissues.

Previous studies suggest that genetic inactivation of ATGL has beneficial effects on the development of metabolic disease. ATGL-deficiency in mice causes a shift from fatty acid to glucose usage in insulin-sensitive tissues which is opposite to that observed in the insulin resistant state[1,9,10]. Interestingly, ATGL-ko mice are also protected from cancer-induced cachexia[19], a complex metabolic disorder characterized by loss of adipose tissue and muscle mass and general physical wasting[20]. In this respect, it is important to note that insulin resistance is present in many cancer patients and may be one mechanism through which muscle wasting occurs[21]. Thus, inhibition of ATGL could help to prevent cancer-associated loss of body mass and insulin resistance. Yet, it is important to note that ATGL-deficiency

causes cardiomyopathy and premature death in humans and rodents due to severe TG accumulation in cardiac muscle[1]. Cardiomyopathy appears to be the only reason for premature death, since ATGL-ko animals overexpressing ATGL exclusively in cardiac muscle exhibit normal life expectancy[22]. It is reasonable to assume that also inhibitor-mediated ablation of ATGL activity can cause cardiac lipid accumulation which limits the potential value of ATGL as therapeutic target. Nevertheless, humans with defective ATGL function reach adulthood and severe cardiac myopathy appears to develop at an age of ~30 years[23] suggesting that myopathy development is slowly progressive. Our experiments suggest that single administration of Atglistatin does not cause cardiac TG accumulation, despite inhibition of lipolysis. On the one hand, this can be explained by transient and incomplete inhibition of ATGL which could avoid ectopic TG accumulation. On the other hand, Atglistatin shows a distinct tissue distribution and primarily accumulates in liver and adipose tissue indicating that the inhibitor does not reach effective concentrations in other tissues.

In summary, our data demonstrate that Atglistatin inhibits lipolysis *in vitro* and *in vivo* by targeting ATGL and hence can serve as a tool compound to study the pathophysiology and druggability of ATGL in animal models of metabolic disease and cachexia.

## Online Methods

### Compound Synthesis

Compounds **1**-**4** were prepared using organic synthesis methods as described in the Supplementary material. Detailed experimental procedures and full characterization data are reported there.

### Expression of recombinant proteins and preparation of cell lysates

Monkey embryonic kidney cells (Cos-7; ATCC CRL-1651) and HEK293T cells were cultivated in DMEM (GIBCO, Invitrogen Corp., Carlsbad, CA), containing 10% fetal calf serum (FCS, Sigma-Aldrich) and antibiotics (100 IU/ml penicillin and 100 μg/ml streptomycin) at standard conditions (37°C, 5% $CO_2$, 95% humidified atmosphere). Cells were transfected with 1 μg DNA complexed to Metafectene (Biontex GmbH, Munich, Germany) in serum free DMEM. After 4 h the medium was replaced by DMEM supplemented with 10% FCS. For the preparation of cell lysates, cells were washed with 1 × PBS, collected using a cell scraper, and disrupted in buffer A (0.25 M sucrose, 1 mM EDTA, 1 mM dithiothreitol, 20 μg/ml leupeptine, 2 μg/ml antipain, 1 μg/ml pepstatin, pH 7.0) by sonication (Virsonic 475, Virtis, Gardiner, NJ). Nuclei and unbroken cells were removed by centrifugation (1,000 × g, 4°C, for 10 min).

For over-expression of ATGL and CGI-58 in *E. coli* (XL-1) cDNA was cloned into the vector pASK-IBA5+ (IBA-BioTagnology). Cells were transformed and cultured overnight at 30°C. Thereafter cells were transferred into a fresh medium and grown until OD600 reached 0.7-0.8. Expression was induced using 0.2 μg/ml anhydrotetracycline. After 3 hours incubation at 37°C cells were harvested, resuspended in lysis buffer (0.25M Sucrose, 1mM DTT, 1mM EDTA) and disrupted by sonication. Lysates were centrifuged at 15,000 g for 20 min at 4°C and the supernatant was collected. Determination of protein concentrations of cell lysates and detection of His-tagged proteins by Western blotting analysis were performed as described below.

### Preparation of tissue homogenates

Murine adipose tissue samples were washed in PBS containing 1 mM EDTA and homogenized on ice in buffer A using an Ultra Turrax (IKA, Staufen, Germany).

Homogenates were centrifuged for 30 min at 20,000 × g and 4°C to obtain tissue extracts. Protein content was determined as described below.

### Determination of TG hydrolase activity

For the determination of TG hydrolase activity of cell lysates containing various recombinant proteins, tissue extracts, or purified proteins, in a total volume of 100 μl buffer A, were incubated with 100 μl substrate in a water bath at 37°C for 60 min. As a control, incubations under identical conditions were performed in buffer A alone. After incubation, the reaction was terminated by adding 3.25 ml of methanol/chloroform/heptane (10:9:7) and 1 ml of 0.1 M potassium carbonate, 0.1 M boric acid, (pH 10.5). After centrifugation (800 × g, 15 min), the radioactivity in 1 ml of the upper phase was determined by liquid scintillation counting. Counts from control incubations were subtracted and the rate of FA hydrolysis calculated using $^{3}H$ radiolabelling of triolein substrate. TG substrate was prepared by emulsifying 330 μM triolein (40 000 cpm/nmol) and 45 μM phosphatidylcholine/phosphatidylinositol (3:1) in 100 mM potassium phosphate buffer, (pH 7.0) by sonication and adjusted to 5 % essentially FA-free BSA (Sigma, St. Louis, MO).

### Determination of MG hydrolase activity

Monoacylglycerol hydrolase activities were determined using recombinant, purified mMGL and *rac*-1-(3)-oleoylglycerol as substrate as described[24].

### Lipolysis of 3T3-L1 cells

3T3-L1 fibroblasts (CL-173) were obtained from ATCC (Teddington, UK) and cultivated in DMEM containing 4.5 g/l glucose and L-glutamine (Invitrogen) supplemented with 10% FCS and antibiotics under standard conditions. Cells were seeded in 12 well plates and two days after confluency medium was changed to DMEM supplemented with 10% FCS containing 10 μg/ml insulin (Sigma-Aldrich), 0.25 μM (0.4 μg/ml) dexamethasone (Sigma-Aldrich), and 500 μM isobutylmethylxanthine (Sigma-Aldrich). After 3 and 5 days, medium was changed to DMEM supplemented with 10% FCS containing 10 μg/ml and 0.5 μg/ml insulin, respectively. On day 7 of differentiation the cells were incubated overnight in the absence of insulin. Cells were used at day 8 of differentiation. For experiments, cells were preincubated with 0, 0.1, 1, 10, or 50 μM of Atglistatin in the presence or absence of 10 μM Hi 76-0079 (*NNC 0076-0000-0079*, provided by Novo Nordisk, Denmark) for 2 h. Then, the medium was replaced by DMEM containing 2% BSA (fatty acid free, Sigma, St. Louis, MO), 20 μM forskolin, and 0, 0.1, 1, 10, or 50 μM of Atglistatin in the presence or absence of 10 μM Hi 76-0079 for 1h. The release of FA and glycerol in the media was determined using commercial kits (NEFA C, WAKO, free glycerol reagent, Sigma). Protein concentration was determined using BCA reagent (Pierce) after extracting total lipids using hexane:isopropanol (3:2), and lysing the cells using 0.3 N NaOH/0.1 % SDS.

### Lipolysis of isolated WAT organ cultures

Gonadal fat pads of wild-type and ATGL-ko mice were surgically removed and washed several times with PBS. Tissue pieces (~15 mg) were preincubated in DMEM containing 0, 0.1, 1, 10, and 50 μM Atglistatin for 8 h at C37°C, 5% $CO_2$, 95% humidified atmosphere. Thereafter, the medium was replaced by DMEM containing 2 % BSA (fatty acid-free) either in the presence or in the absence of 20 μM forskolin and 0, 0.1, 1, 10, and 50 μM, and incubated for another 60 min at 37°C. Then, aliquots of the medium were collected and analyzed for FA and glycerol content using commercial kits (HR Series NEFA-HR(2), WAKO Diagnostics, Neuss, Germany; Sigma, St. Louis, MO). For protein determinations, fat pads were washed extensively with PBS and lysed in 0.3 N NaOH/0.1 % SDS. Protein measurements were performed using the BCA reagent (Pierce Rockfort, IL).

### Toxicity test for Atglistatin in AML-12 mouse hepatocytes

For MTT-based *in vitro* viability assays, cells were seeded at an initial density of $1\times10^4$ cells per well in 96-well plates and cultured under standard conditions for 24 hours. The next day, cells were pretreated with different concentrations of Atglistatin dissolved in DMSO or Cisplatin dissolved in dimethylformamide (DMF) (Sigma-Aldrich) as positive control for two hours. Medium was replaced by an identical fresh medium and incubated again for the indicated time-points. Thereafter cells were incubated for 3 hours with 100 μl Thiazolyl Blue Tetrazolium Bromide (MTT). The resulting violet formazan crystals were dissolved by adding 100 μl of MTT solubilization solution (0.1% NP-40, 4 mM HCl and anhydrous isopropanol). After complete dissolution of the formazan product, absorbance was measured at 595 nm using 690 nm as reference wavelength.

### Animals

Mice (C57Bl/6J) were maintained on a regular light-dark cycle (14 hours light, 10 hours dark) and kept on a standard laboratory chow diet (4.5% wt/wt fat, Sniff GMBH Germany). Maintenance, handling, and tissue collection from mice has been approved by the Austrian Federal Ministry for Science and Research and by the ethics committee of the University of Graz.

### Inhibitor administration

Atglistatin was administrated orally by gavage in olive oil (200 μl) or by IP injection. For IP administration, we generated Atglistatin hydrochloride by the addition of 25 % HCl resulting in a water soluble compound. For intraperitoneal injection the inhibitor was dried, excess HCl was buffered with Tris base, and Atglistatin was dissolved in PBS containing 0.25 % Cremophor® EL (pH 7.1; Sigma Chemical Co.).

### Determination of tissue TG content

For tissue collection mice were sacrificed by cervical dislocation. Subsequently, tissues were excised and snap frozen. After homogenisation in buffer A, neutral lipids were extracted by the Folch method. Total lipid extracts were reconstituted in 2 % Triton X-100 and TG content was measured using TG reagent (Thermo Electron Corp., Victoria, Australia).

### Determination of lysophospholipase activity

Lysophospholipase activity of PNPLA 6 and PNPLA 7 was performed as previously described [25]. In brief, lysates of COS-7 cells overexpressing PNPLA6, PNPLA7 or LacZ were incubated with 3 mM 1-oleoylglycerophospholcholine at 37°C for 20 min in the absence or presence of Atglistatin (0 – 100 μM). The assay was terminated by heat inactivation at 75°C and the release of free fatty acids was measured with a colorimetric kit (Wako Diagnostics) according to the manufacturer's instructions.

### Tissue distribution of Atglistatin

Atglistatin was administered orally by gavage in olive oil (1.4 mg/mouse). After 8 h tissues were collected and extracted twice using Folch procedure. Combined organic phases were concentrated, reconstituted in 500μl chloroform and ssubjected to solid phase extraction (SPE). For SPE samples were loaded onto silica columns washed twice with 2 ml of chloroform and Atglistatin was eluted using 3 ml chloroform/methanol (99/1, v/v). Eluted samples were concentrated, dissolved in n-propanol/chloroform/methanol (8/1.3/0.6, v/v/v) and analyzed by UPLC/MS (m/z 284, MH+; SYNAPT™ G1 qTOF HD mass spectrometer, Waters).

Europe PMC Funders Author Manuscripts

### Co-immunoprecipitation of ATGL and CGI-58

Flag-tagged ATGL or empty Flag vector were cotransfected into HEK293T cells with either His-tagged LacZ (Beta-galactosidase) or His-tagged CGI-58. 24 h after transfection cells were harvested using a cell scraper and lysed in buffer C (50 mM Tris-Cl, pH 7.4, 150 mM NaCl, 1 mM EDTA, 1 % NP40) on ice. After centrifugation (1000 g, 4°C, 10 min) the supernatant (0.5 mg protein) was incubated with 10 μl anti-flag-agarose (Sigma) over night at 4°C under shaking. After 5 washing steps in buffer C the flag-agarose was heated to 99°C for 10 min in 2 × SDS sample buffer. Thereafter the input and the immunoprecipitated fraction where subjected to SDS-PAGE and Flag and His tagged proteins where detected using flag-, and his-antibodies.

### Lipid droplet isolation from adipocytes

White adipose tissue lysates of wild type and ATGL deficient (ATGL-ko) mice were incubated in the presence or absence of 40 μM Atglistatin for 15 min at room temperature under constant shaking. Alternatively, 3T3-L1 adipocytes were incubated for 3 h in the presence or in the absence of 40 μM Atglistatin and cells were harvested using a cell scraper and disrupted by sonication. LDs and cytosolic fractions from tissue- and 3T3-L1 cell lysates where isolated by differential centrifugation in a sucrose gradient for 1 h at 100,000 g. LDs where collected as a white band from the top of the tube and washed in buffer A by another centrifugation step for 1 h at 100,000 × g. Total fractions, lipid droplets, and cytosolic fraction of 3T3-L1 adipocytes as well as of wild-type and of ATGL-ko white adipose tissue were subjected to western blotting analysis using antibodies specific for murine ATGL, perilipin 1, and GAPDH (Glycerinaldehyde 3-phosphate dehydrogenase) and the respective secondary antibodies.

### Plasma parameters

Blood samples of fed or fasted mice were collected by retro-orbital puncture. Plasma levels of TG, glycerol, FA, and total cholesterol were determined using commercial kits (Thermo Electron Corp., Victoria, Australia; Sigma, St. Louis, MO; Wako Chemicals, Wako Chemicals, Neuss, Germany; Roche Diagnostics, Vienna, Austria). Blood glucose was determined using Accu-Check glucometer (Roche, Diagnostics).

### Determination of protein concentrations

Protein concentrations were determined using Bio-Rad protein assay according to the manufacturer's protocol (Bio-Rad 785, Bio-Rad Laboratories, Munich, Germany), using BSA as standard. Alternatively, protein measurements were performed using the BCA reagent (Pierce, Rockford, IL).

### Statistical Analysis

Statistical analyses were determined by Student's unpaired *t*-test (two tailed). Following levels of statistical significance were used: $*p < 0.05$, $**p < 0.01$, and $***p < 0.001$.

## Supplementary Material

Refer to Web version on PubMed Central for supplementary material.

## Acknowledgments

This work was supported by the doctoral program W901-B05 DK Molecular Enzymology (Ro. Zi., R. B.), Translational Program (grant no. TRP4, Ro. Zi.), and the Wittgenstein Award 2007 (grant no. Z136, Ru. Ze.) funded by the Austrian Science Fund (FWF), and GOLD, Genomics of Lipid-Associated Disorders (Ru. Ze., Ro. Zi.), and PLACEBO, Platform for Chemical Biology in Austria (R. B.), as part of the Austrian Genome Project

GEN-AU funded by the Forschungsförderungsgesellschaft und Bundesministerium für Wissenschaft und Forschung. We are grateful to Bettina Grumm and Bernhard Wölfl for skilful help in the synthesis of Atglistatin. Furthermore, we thank P. Jacobsen, and H. Tornqvist from Novo Nordisk for helpful discussions and for the provision of lead compounds.

## Abbreviations

| | |
|---|---|
| **ATGL** | adipose triglyceride lipase |
| **CGI-58** | comparative gene identification-58 |
| **DG** | diacylglycerol |
| **FA** | fatty acid |
| **FCS** | fetal calf serum |
| **HSL** | hormone-sensitive lipase |
| **LD** | lipid droplet |
| **MGL** | monoglyceride lipase |
| **MTT** | Thiazolyl Blue Tetrazolium Bromide |
| **NLSD** | Neutral Lipid Storage Disease |
| **PPAR** | peroxisome proliferator-activated receptor |
| **TC** | total cholesterol |
| **TG** | triacylglycerol |
| **WAT** | white adipose tissue |

## References

1. Haemmerle G, et al. Defective lipolysis and altered energy metabolism in mice lacking adipose triglyceride lipase. Science. 2006; 312:734–737. [PubMed: 16675698]
2. Lass A, et al. Adipose triglyceride lipase-mediated lipolysis of cellular fat stores is activated by CGI-58 and defective in Chanarin-Dorfman Syndrome. Cell Metab. 2006; 3:309–319. [PubMed: 16679289]
3. Zimmermann R, et al. Fat mobilization in adipose tissue is promoted by adipose triglyceride lipase. Science. 2004; 306:1383–1386. [PubMed: 15550674]
4. Fredrikson G, Tornqvist H, Belfrage P. Hormone-sensitive lipase and monoacylglycerol lipase are both required for complete degradation of adipocyte triacylglycerol. Biochim. Biophys. Acta. 1986; 876:288–293. [PubMed: 3955067]
5. Zimmermann R, Lass A, Haemmerle G, Zechner R. Fate of fat: the role of adipose triglyceride lipase in lipolysis. Biochim. Biophys. Acta. 2009; 1791:494–500. [PubMed: 19010445]
6. Boden G. Obesity, insulin resistance and free fatty acids. Curr. Opin. Endocrinol. Diabetes Obes. 2011; 18:139–143. [PubMed: 21297467]
7. Carobbio S, Rodriguez-Cuenca S, Vidal-Puig A. Origins of metabolic complications in obesity: ectopic fat accumulation. The importance of the qualitative aspect of lipotoxicity. Curr. Opin. Clin. Nutr. Metab. Care. 2011; 14:520–526. [PubMed: 21849895]
8. Schaffer JE. Lipotoxicity: when tissues overeat. Curr. Opin. Lipidol. 2003; 14:281–287. [PubMed: 12840659]
9. Kienesberger PC, et al. Adipose triglyceride lipase deficiency causes tissue-specific changes in insulin signaling. J. Biol. Chem. 2009; 284:30218–30229. [PubMed: 19723629]
10. Hoy AJ, et al. Adipose triglyceride lipase-null mice are resistant to high-fat diet-induced insulin resistance despite reduced energy expenditure and ectopic lipid accumulation. Endocrinology. 2010; 152:48–58. [PubMed: 21106876]

11. Ong KT, Mashek MT, Bu S, Mashek DG. Hepatic ATGL knockdown uncouples glucose intolerance from liver TAG accumulation. FASEB J. 2013; 27:313–321. [PubMed: 22993196]
12. Li LO, Klett EL, Coleman RA. Acyl-CoA synthesis, lipid metabolism and lipotoxicity. Biochim. Biophys. Acta. 2010; 1801:246–251. [PubMed: 19818872]
13. Summers SA. Ceramides in insulin resistance and lipotoxicity. Prog. Lipid Res. 2006; 45:42–72. [PubMed: 16445986]
14. Samuel VT, Petersen KF, Shulman GI. Lipid-induced insulin resistance: unravelling the mechanism. Lancet. 2010; 375:2267–2277. [PubMed: 20609972]
15. Ebdrup S, Sorensen LG, Olsen OH, Jacobsen P. Synthesis and structure-activity relationship for a novel class of potent and selective carbamoyl-triazole based inhibitors of hormone sensitive lipase. J. Med. Chem. 2004; 47:400–410. [PubMed: 14711311]
16. Ebdrup S, Refsgaard HH, Fledelius C, Jacobsen P. Synthesis and structure-activity relationship for a novel class of potent and selective carbamate-based inhibitors of hormone selective lipase with acute in vivo antilipolytic effects. J. Med. Chem. 2007; 50:5449–5456. [PubMed: 17918819]
17. Schweiger M, et al. Adipose triglyceride lipase and hormone-sensitive lipase are the major enzymes in adipose tissue triacylglycerol catabolism. J. Biol. Chem. 2006; 281:40236–40241. [PubMed: 17074755]
18. Wilson PA, Gardner SD, Lambie NM, Commans SA, Crowther DJ. Characterization of the human patatin-like phospholipase family. J. Lipid Res. 2006; 47:1940–1949. [PubMed: 16799181]
19. Das SK, et al. Adipose triglyceride lipase contributes to cancer-associated cachexia. Science. 2011; 333:233–238. [PubMed: 21680814]
20. Tisdale MJ. Cancer cachexia. Curr. Opin. Gastroenterol. 2010; 26:146–151. [PubMed: 19918173]
21. Honors MA, Kinzig KP. The role of insulin resistance in the development of muscle wasting during cancer cachexia. J. Cachexia Sarcopenia Muscle. 2012; 3:5–11. [PubMed: 22450024]
22. Haemmerle G, et al. ATGL-mediated fat catabolism regulates cardiac mitochondrial function via PPAR-alpha and PGC-1. Nat. Med. 2011; 17:1076–1085. [PubMed: 21857651]
23. Hirano K. A novel clinical entity: triglyceride deposit cardiomyovasculopathy. J. Atheroscler. Thromb. 2009; 16:702–705. [PubMed: 19729869]
24. Taschler U, et al. Monoglyceride lipase deficiency in mice impairs lipolysis and attenuates diet-induced insulin resistance. J. Biol. Chem. 2011; 286:17467–17477. [PubMed: 21454566]
25. Kienesberger PC, et al. Identification of an insulin-regulated lysophospholipase with homology to neuropathy target esterase. J. Biol. Chem. 2008; 283:5908–5917. [PubMed: 18086666]


Europe PMC Funders Author Manuscripts

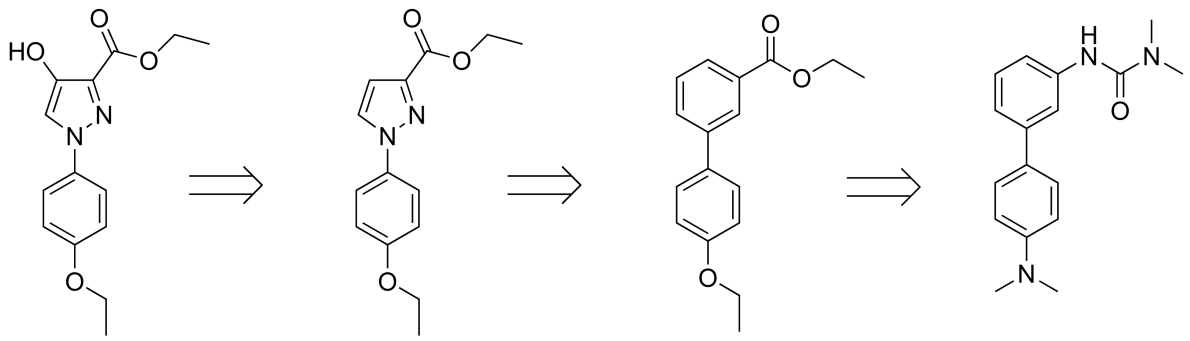

| | 1 | 2 | 3 | 4 |
|---|---|---|---|---|
| **$IC_{50}$ (μM):** | 50 +/- 10 | 40 +/- 8 | 12 +/- 3 | 0.7 +/- 0.1 |



Europe PMC Funders Author Manuscripts

Europe PMC Funders Author Manuscripts

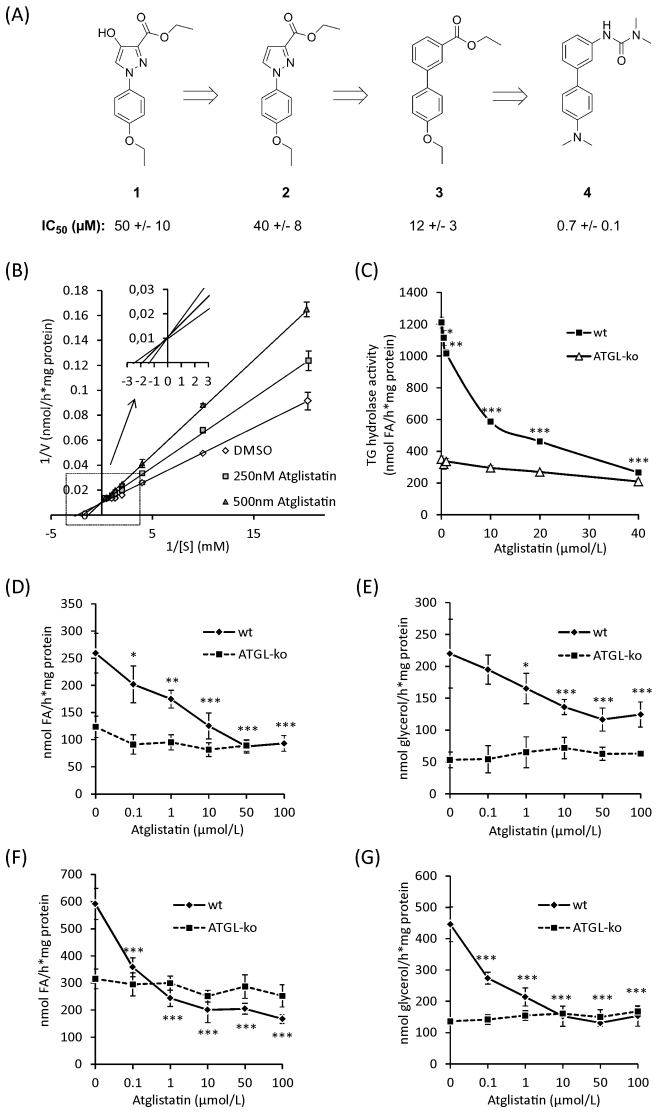


**Fig. 1. Development of ATGL inhibitors and inhibition of lipolysis *in vitro***

For determination of lipase activity, lysates from E. *coli* overexpressing ATGL and CGI-58 (A, B) or WAT (C) were incubated with a substrate containing radiolabeled [9,10-$^3$H(N)]-triolein. Liberated FA were extracted and quantitated by liquid scintilation. Inhibitors were dissolved in DMSO and DMSO alone was used as negative control. **(A)** Structure and $IC_{50}$ values of compounds **1**-**4. (B)** Lineweaver-Burk plot for kinetic analysis of ATGL inhibition. Experiments were performed at varying concentrations of substrate (0.05 - 1 mM) in presence and absence of compound **4** (Atglistatin). The insert shows the intersection with the y- and x-axis representing $1/V_{max}$ and $-1/K_m$, respectively. **(C)** Dose-dependent inhibition of TG hydrolase activity in WAT lysates obtained from wild-type and ATGL-ko mice. **(D-G)** Effect of Atglistatin on basal (D, E) and forskolin-stimulated (F, G) FA and glycerol release in WAT organ cultures. WAT pieces (~15 mg, $n$=5 for each concentration) of wild-type or ATGL-ko mice were cultured for 8 h in DMEM containing 2 % FA-free BSA and the indicated concentrations of Atglistatin. Subsequently, the medium was replaced by identical fresh medium and samples were collected after incubation for another hour in the presence or absence of inhibitor and/or forskolin. FA and glycerol release was

determined using commercial kits. Data are presented as mean ± S.D. (*, $p < 0.05$ **, $p < 0.01$; ***, $p < 0.001$) and representative for at least three independent experiments.



Europe PMC Funders Author Manuscripts

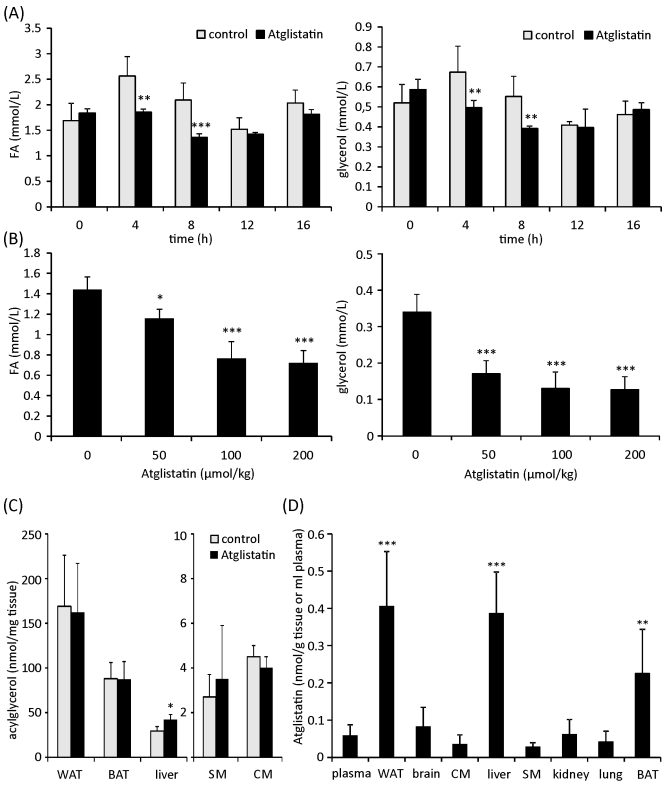


**Fig. 2. Inhibition of lipolysis *in vivo* and tissue distribution of Atglistatin**

The inhibitor was dissolved in olive oil and applied by oral gavage to over-night fasted C57Bl6 mice. Olive oil alone served as a control. Blood was taken retro-orbitally and plasma parameters were measured using commercial kits. (**A**) Time-dependent effect of Atglistatin (200 µmol/kg). (**B**) Dose-dependent effect of Atglistatin (8 h after application). (**C**) Tissue TG levels (8 h after application of 200 µmol/kg). (**D**) Tissue distribution of Atglistatin (8 h after application of 200 µmol/kg). For (C) and (D), tissues were collected and extracted twice using the Folch procedure. The organic phase was evaporated and lipids were reconstituted in 2% Triton for enzymatic determination of tissue TG levels. For the determination of Atglistatin concentrations, organic phases were concentrated, reconstituted in chloroform, and subjected to solid phase extraction (SPE) using silica columns. After loading, columns were washed twice with 2 ml of chloroform and Atglistatin was eluted using 3 ml chloroform/methanol (99/1, v/v). Eluted samples were concentrated, resolved in npropanol/chloroform/methanol (8/1,3/0,6, v/v/v) and analyzed using UPLC/ MS (m/z 284, MH+). Data are presented as mean of 5-6 animals ± S.D. The amount of Atglistatin in various tissues was statistically compared to that in plasma (**, p < 0.05 **, p < 0.01; ***, p < 0.001).*




Europe PMC Funders Author Manuscripts